Failure analysis on cracking and leakage of 304 stainless steel flange in petrochemical butyl device

Failure analysis on cracking and leakage of 304 stainless steel flange in petrochemical butyl device

Lei Cheng[1], Chenyang Du[1*], Xiaowei Li[1], Baolin Liu[1] and Guoju Cui[2]

[1]China Special Equipment Inspection and Research Institute, Beijing 100029, China.
[2]SINOPEC Shengli Oilfield Company Petrochemical Plant, Dongying 257001, China.

[*]chenyangdu@126.com

Abstract: During the pressure test process in a petrochemical butyl device in China, it was found that the 304 stainless steel flange of the ethylene pipeline appeared to be cracking and leakage. This article analyzed the reasons for failure using macroscopic inspection, chemical composition analysis, metallographic structure analysis, scanning electron microscope, energy dispersive spectroscopy, mechanical properties test, and intergranular corrosion test. The results show that the carbon content of the flange base material exceeds the standard, many carbides precipitate at the grain boundary, the material itself is seriously sensitized, and the intergranular corrosion resistance is reduced. At the same time, under corrosive media such as sulfur and chlorine and high stress, the flange displays stress corrosion cracking, which leads to cracking and leakage failure. This article reports the reasons for the failure of the flange, and some reasonable suggestions are put forward to avoid similar leakage accidents.

1 Introduction

As a kind of synthetic rubber, butyl rubber possesses good wear resistance and high damping [1], which is mainly used to manufacture automotive tires, sealing elements, vulcanized capsules, shock-absorbing support fields, etc [2, 3]. Due to excellent corrosion resistance, mechanical properties, machinability, and weldability, 304 austenitic stainless steel is generally adopted as a flange material in synthetic rubber synthesis devices [4]. Although 304 austenitic stainless steel has many advantages, it is prone to stress corrosion in the industrial environment containing sulfur and chlorine media, which may result in cracking and leakage failure of petrochemical equipment. Therefore, performing an analysis to clarify the reasons for failure is an important route to take preventive measures to avoid the recurrence of failure and improve quality reliability.

There is an actual instance of cracking and leakage failure of 304 stainless steel flange in a petrochemical butyl device. During the pressure test process in a petrochemical synthetic rubber factory in China, it was found that the flange of the ethylene pipeline appeared to be cracking and leakage, which caused the pressure test to be interrupted. The elementary information on the failure flange is illustrated below. This flange was used in 2005 and was made of 304 austenitic stainless steel. Its specification was DN50, operation pressure was 1.8MPa, and operation temperature was -35 ℃. The working medium was ethylene. The wall thickness grade and connecting pipe value were sch40s and 7.1 mm.

This paper sampled materials in intact and cracked areas of 304 stainless steel to perform related physical and chemical performance testing. With the tests of chemical composition, metallographic analysis, scanning electron microscopy (SEM) with energy dispersive spectrum (EDS) analysis,

mechanical properties test, and intergranular corrosion test, the reasons for cracking and leakage failure of 304 stainless steel flange in petrochemical butyl device is determined and the relevant protection suggestions are further put forward.

2 Physical and chemical experiments characterization of flange failure

2.1 Macroscopic examination

Firstly, the failure flange was observed macroscopically, and the macroscopic failure characteristics of the failure flange were mastered, which laid a good foundation for the subsequent experimental analysis. Figure 1 and Figure 2 are the macroscopic of flange crack morphology. Macro-inspection indicates no obvious corrosion on the inner and outer surfaces. The cracks are distributed along the circumference of the flange neck in a zigzag and intermittent way, almost parallel to the weld. The cracks on the outer surface of the flange neck are extended in a full circle along the circumferential direction, and some of them have penetrated. Besides, it is displayed that the crack gap on the outer surface is larger than on the inner surface. Considering that the crack position is not only a structural discontinuity but also a weld heat-affected zone with high-stress characteristics, it can be judged from the foregoing phenomena that the cracks originate from the outer surface and extend to the inner surface.

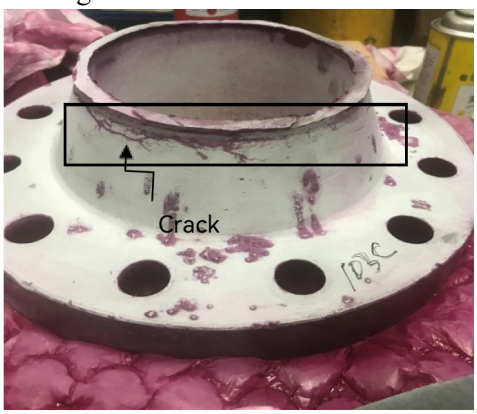

Figure 1. External crack morphology of flange.

Figure 2. Morphology of internal cracks in flange.

2.2 Material chemical composition analysis

Next, the chemical composition of the material is analyzed to check whether the flange material meets the relevant design and manufacturing requirements. The specimens far away from the cracked location are sampled to verify whether the chemical composition of the flange is reasonable. Table 1 shows the results of the chemical composition elements analysis. Compared with the measured value in the Chinese NB/T 47010-2017 standard, the results indicate that the C content is 0.16%, which is larger than the upper limit of the standard value, while the Cr content is 16.66%, which is lower than the lower limit of the standard value. Due to Cr, Ni is an essential corrosion-resistant element of stainless steel. Cr can be formed on the surface of the stainless steel chromium-rich oxide film, which effectively protects the stainless steel from the medium of further Oxidation and corrosion and improves the corrosion resistance of stainless steel [5, 6]. Consequently, this flange possesses the chemical composition features of high-carbon and low-Cr, which may lead to decreased intergranular corrosion resistance and increased sensitization possibility.

Table 1. Chemical composition analysis of flange material (wt.%).

Element	C	Cr	Ni	Mn	S	P
Standard value (NB/T47010-2017)	≤0.08	18.00~20.00	8.00~11.00	≤2.00	≤0.03	≤0.045
Measured value	0.16	16.66	9.03	0.75	0.01	0.02

2.3 Metallographic analysis

Metallographic analysis was carried out to observe the microstructure characteristics of the crack. Figure 3 displays the microscopic metallographic morphology of flange cracks. It can be seen the microstructure is austenite, and there are twins and granular carbides distributed in the grain, which leads to a significant electrochemical property difference between the grain and the grain boundary. Besides, the cracks display dendritic morphology with obvious trunk and branches and spread along the grain boundary with sharp tips, which is a typical feature of stress corrosion cracking.

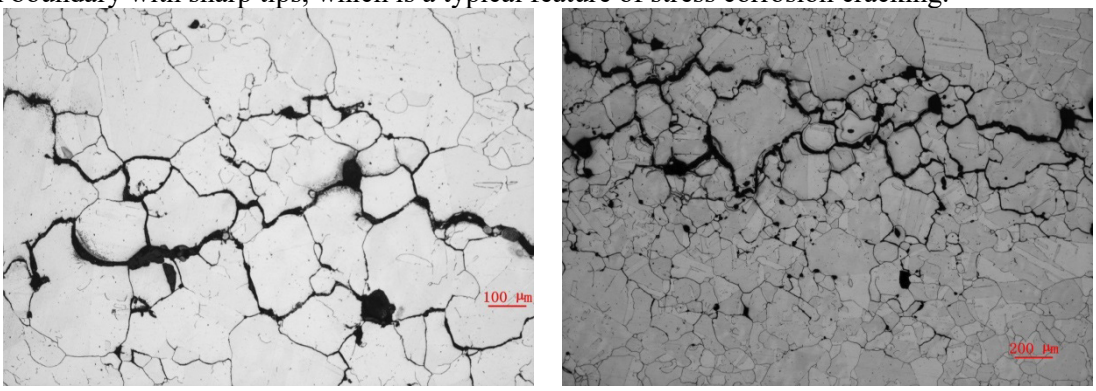

Figure 3. Microscopic morphology of cracks.

2.4 SEM and EDS analysis

SEM and EDS were used to analyze the crack position of the flange, and the micro-morphology characteristics of the crack position were observed. The corresponding corrosion element information was found. As shown in Figure 4, the fracture surface of the flange was further observed with SEM. The results illustrate that the fracture surfaces have a polyhedral feature and crystalline grains are angular and smooth to show a typical rock sugar shape. The results reveal that the flange cracking is an obvious intergranular fracture. Table 2 exhibits the energy spectrum analysis results of the corrosion products on the fracture surface. Compared with the chemical composition result in Table 1, the contents of chlorine and sulfur increase significantly, respectively, at 3.02% and 0.49%. This may be attributed to the fact that there are many corrosive elements in the industrial environment, and the increase in sulfur and chlorine content is related to the exposed contact between the flange and the atmospheric environment. The increase of chloride and sulfur contents will destroy the passive film formed on the grain boundary, resulting in intergranular corrosion or pitting corrosion and easily causing stress corrosion cracking of the flange.

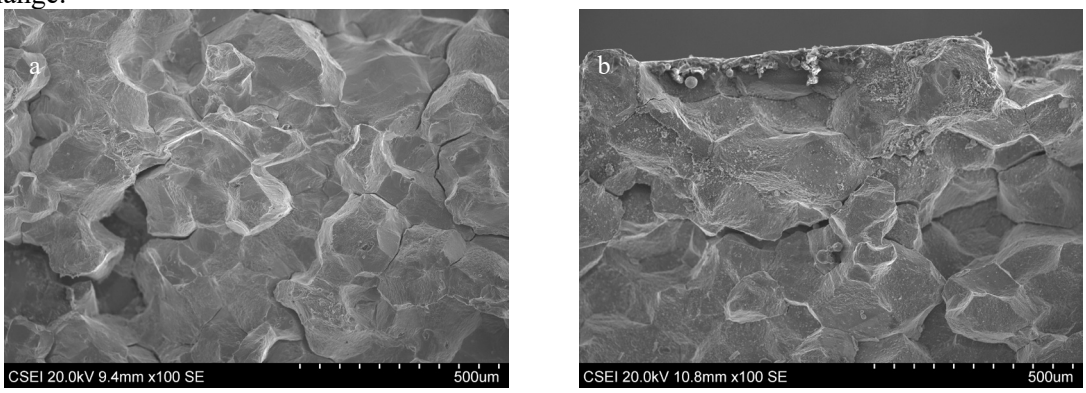

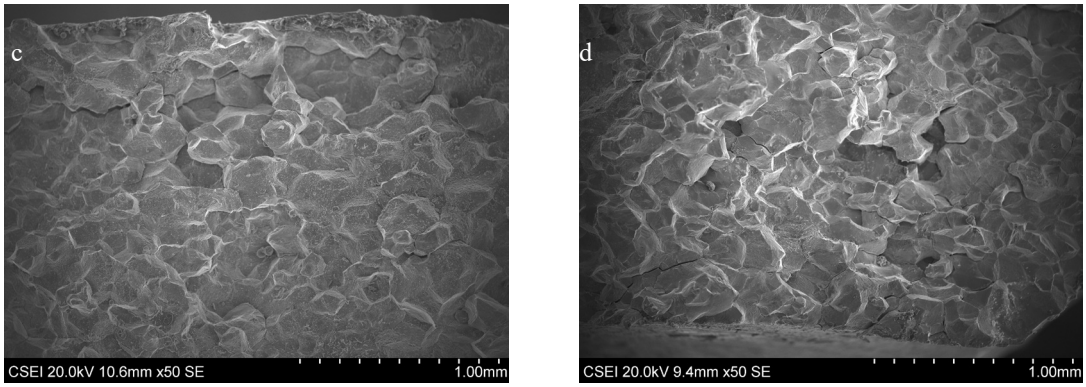

Figure 4. Fracture morphology of flange.

Table 2. Content of elements in energy spectrum analysis of corrosion products

Element	Mass/%	Atom/%
C	34.44	50.46
O	35.86	39.44
S	0.49	0.27
Cl	3.02	1.50
Cr	3.66	1.24
Fe	22.22	7.00

2.5 Mechanical properties and intergranular corrosion tests

The mechanical properties of the failed flange were tested, and the mechanical properties of the current materials were mastered. The samples from the flange cracks were taken for impact and tensile tests, respectively. Tables 3 and 4 are the test results corresponding to the aforementioned tests, respectively. It can be seen that the mechanical indexes such as impact absorption energy, yield strength, tensile strength, and area shrinkage all meet the requirements of China NB/T 47010-2017 standard.

Table 3. Impact test results.

Sample No.	Sample size/mm	Test temperature/℃	Impact absorbing energy/J
1	9.98×9.99×55	23	217
2	9.98×9.99×55	23	228

Table 4. Tensile test results.

Sample No.	Lu/mm	Yield strength Rp0.2/MPa	Tensile strength Rm/MPa	Reduction of area A/%
1	38.47	355	663	54.0
2	37.49	367	664	50.0

Samples were taken at the crack and the base of the flange, and intergranular corrosion tests were carried out to determine whether the stainless steel material of the flange was sensitized. As indicated in Figure 5, it can be seen that there are a lot of carbides precipitated at the grain boundary accompanied by pitting corrosion, and corrosion grooves surround some grains. According to GB/T 4334-2020, it can be judged as three types of groove structure, and the material itself is seriously sensitized. The possible

reasons for sensitization may be that the flange has not been treated by a solid solution process before leaving the manufacturing plant.

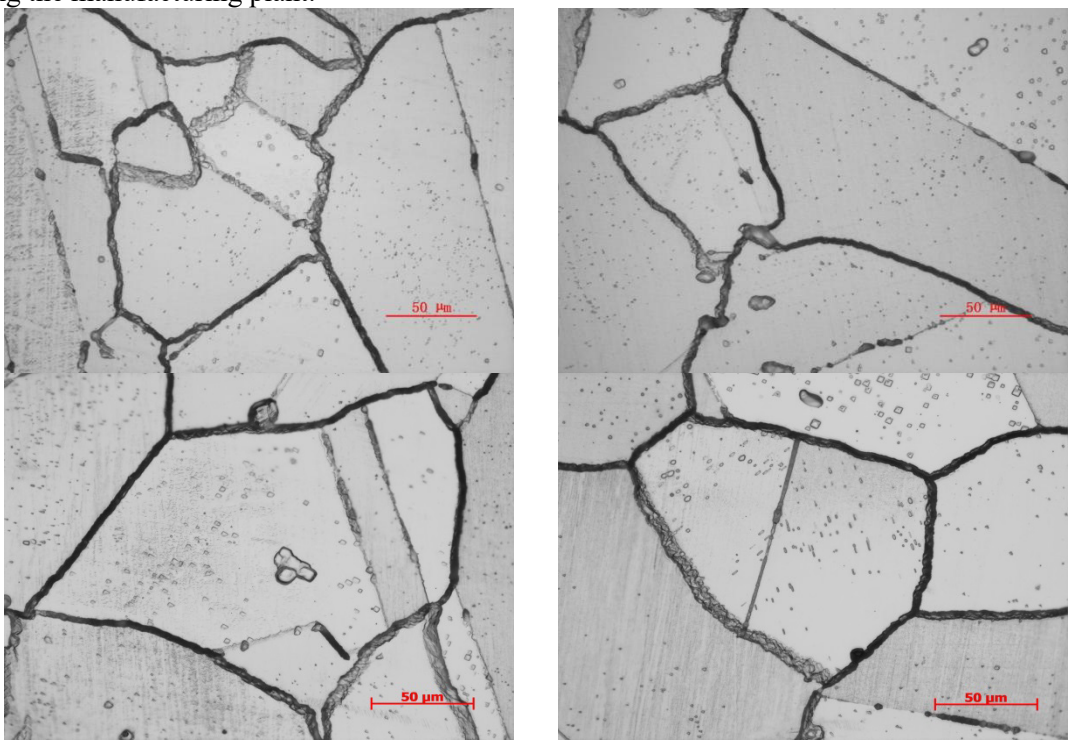

Figure 5. Morphology of intergranular corrosion.

3 Analysis and discussion

Based on the above physical and chemical inspection results, the flange cracking failure is analyzed as follows.

3.1 Sensitive materials

According to material chemical composition analysis, the chemical composition of the element is beyond the limits of related standards. The carbon content is higher than the maximum value, and the chromium content is lower than the minimum value specified in the standard. At the same time, there are a lot of carbides precipitated on the grain boundary of the flange microstructure, which is related to the high carbon content of the flange and the hot working process system. Excessive carbon element provides a material basis for generating grain boundary precipitates.

The higher the carbon content, the higher the sensitization sensitivity, the greater the tendency of intergranular carbide precipitation, and the more prone to intergranular corrosion [7, 8]. It is well known that if the carbon content in stainless steel is lower than 0.08%, the amount of carbide precipitation is less; if the carbon content is higher than 0.08%, the amount of carbide precipitation will increase rapidly [9]. Besides, the solubility of carbon in austenite at room temperature is very small, at only about 0.02%; thus, supersaturated carbon is dissolved in austenite [10]. After solution treatment, when the temperature stays in the range of 450-850℃ for some time, the supersaturated carbon continuously diffuses to the austenite grain boundary. It combines with chromium to form $Cr_{23}C_6$ compounds. Because the diffusion speed of chromium in grains is slower than that along grain boundaries, the internal chromium can't diffuse to grain boundaries. The chromium needed for chromium carbide formed between grains mainly comes from the vicinity of grain boundaries, greatly reducing the chromium content near grain boundaries. When the chromium content at grain boundaries is less than 12%, it forms a chromium-poor region and causes a sensitizing phenomenon [11].

The above process is further validated by the results of the intergranular corrosion test, which shows that the flange material itself has been seriously sensitized. The occurrence of sensitization leads to a significant difference in electrochemical performance between the chromium-poor region and the crystal grain itself, which further forms an activated-passive battery with great potential difference between the chromium-poor region (anode) and the substrate (cathode). The chromium-poor area at the grain boundary is rapidly corroded with corrosive media such as sulfur and chlorine combined in the atmospheric environment. Consequently, the intergranular bonding force is significantly weakened, and the grain boundary's mechanical strength and intergranular corrosion resistance are significantly reduced [12-14].

3.2 Specific corrosive medium

Energy spectrum analysis shows that the corrosion products on the fracture surface contain corrosive elements such as chlorine, sulfur, oxygen and matrix elements such as iron and chromium. The appearance of corrosive elements is related to the direct contact between the flange and the atmospheric environment, the erosion of rain, and the existence of this element in the atmospheric environment of the factory.

3.3 Welding residual stresses

In the process of flange welding, due to the physical properties of austenitic stainless steel itself, the thermal conductivity is small, and the linear expansion coefficient is large. Significant welding residual stresses will be generated in the heat-affected zone of the welding process [15, 16], which provides conditions for intergranular stress cracking.

From the above analysis, it can be seen that the flange neck cracking meets the three conditions of stress corrosion cracking. Under normal circumstances, stress corrosion cracking of austenitic stainless steel caused by chloride ions is intergranular [17, 18]. When there is a precipitated phase of carbides such as $Cr_{23}C_6$ on the grain boundary of austenitic stainless steel, the electrode potential of the precipitate is different from that of solid solution austenitic grain, which is easy to form many micro-batteries. With the precipitation of chromium, the austenite grain boundary has a lower potential. It forms the anode of the micro-battery, so the grain boundary becomes the preferential channel for corrosion. At the same time, the crack opens under stress, accelerating the crack propagation, and finally, the intergranular stress corrosion cracking morphology is produced.

4 Conclusions and recommendations

This article reports the cracking and leakage failure analysis of 304 stainless steel flange in a petrochemical butyl device. The chemical composition of the flange material is unqualified. The content of C is higher than the upper limit, while the content of Cr is lower than the lower limit of the standard values. Serious sensitization occurs, displaying that a large number of carbon and chromium compounds are precipitated on the grain boundary, which reduces the grain boundary strength and corrosion resistance, and there is an obvious tendency for intergranular corrosion. Under the combined action of corrosive media such as sulfur and chlorine in an atmospheric environment and high welding residual stress, intergranular corrosion occurs in the welding heat-affected zone, which results in flange fracture failure with typical stress corrosion cracking. The problems found in this failure analysis should also attract the attention of enterprise managers. The reinspection of incoming materials is the first checkpoint to control the quality. If we don't pay attention to it, it will lead to many subsequent problems.

Based on the above analysis, preventive measures and effective suggestions are provided to avoid recurrence failure for other flanges. Firstly, newly purchased 304 stainless steel flanges should be treated by solution treatment after forging; thus, the carbides dissolve in austenite after heating to 1100-1150°C, and then they are rapidly cooled to obtain a single-phase austenite structure. The ultra-low carbon 304L covered electrode is used for welding, such as A002, etc, which can avoid the precipitation of weld carbide during welding. Secondly, the quality of materials can be controlled by

strengthening the supervision of incoming flange materials through related tests, such as chemical composition analysis, metallographic examination, and intergranular corrosion test. Thirdly, the interlayer temperature of weldments should be kept low, preferably not exceeding 150℃. During field welding, the residence time at 450-850℃ can be reduced by shortening the heating time, reducing the weld cross-section, reducing the linear energy, and cooling rapidly to avoid the material sensitization caused by welding.

References

[1] Shen, M., Xia, L., Feng, Q., Zhang, J., Li, J., Guo, S. Damping characteristics of a multilayered constrained beam using viscoelastic butyl rubber layer with wide temperature range. Mater. Express, 2021, 11 (3),372-380.
[2] Shiva, M, Kamkar Dallakeh, M, Ahmadi, M, Lakhi, M. Effects of silicon carbide as a heat conductive filler in butyl rubber for bladder tire curing applications. Marer Today Commun, 2021, 29,102773.
[3] Lee, S. R., Bae, K. M., Baek, J. J., Kang, M. C., Lee, T. I. Adhesion enhancement between aluminum and butyl rubber by (3-mercaptopropyl) trimethoxy silane for vibration damping plate. J. Adhesion Sci. Technol,2021,35 (10),1114-1124.
[4] Sharma R. K., Mohanty S., Gupta V. Advances in butyl rubber synthesis via cationic polymerization: An Overview [J]. Polymer International. 2021.DOI:10.1002/pi.6180.
[5] Sun, J., Tang, H., Wang, C., Han, Z. & Li, S. (2022). Effects of alloying elements and microstructure on stainless steel corrosion: A review. steel research international, 93(5),2100450.
[6] Sun, M., Du, C., Liu, Z., Liu, C., Li, X. & Wu, Y. (2021). Fundamental understanding on the effect of Cr on corrosion resistance of weathering steel in simulated tropical marine atmosphere. Corrosion science, 186, 109427.
[7] Shit, G., Mariappan, K. & Ningshen, S. (2023). Improvement of sensitization and intergranular corrosion of AISI type 304L stainless steel through thermo-mechanical treatment. Corrosion Science, 213, 110975.
[8] Bai, S., Zhang, S., Ma, J., Li, J., & Mou, L. (2024). Understanding the effect of decreasing C contents and increasing solid-solution time on intergranular corrosion resistance of 304 austenitic stainless steel. Journal of Materials Research and Technology, 30, 4750-4761.
[9] Hwang E. R., Kang, S. G. Intergranular corrosion of stainless steel in molten carbonate salt [J]. Journal of Materials Science Letters,1997,16 (16): 1387- 1388.
[10] Bi H. J. Influence of heat treatment to microstructures and localized corrosion in several stainless steels [D]. Lanzhou: Lanzhou University of Technology. 2011.
[11] Marikkannan, S. K., Gnanasekaran, S., Rakkiyannan, J., Veluchamy, M., Subramanian, P. & Sujatha, V. I. (2023, July). Heat treatment effect on sensitization behavior of 304 grade stainless steel. In AIP Conference Proceedings (Vol. 2788, No. 1). AIP Publishing.
[12] Fujii, T., Kawarabayashi, K. & Shimamura, Y. (2024). Intergranular corrosion in sensitized austenitic stainless steel subjected to tensile loading and unloading in the elastic-plastic region. Corrosion Science, 230, 111896.
[13] Vukkum, V. B., Delvecchio, E., Christudasjustus, J., Storck, S. & Gupta, R. K. (2023). Intergranular Corrosion of Feedstock Modified—Additively Manufactured Stainless Steel After Sensitization. Corrosion, 79(PNNL-SA-186235).
[14] Zatkalíková, V., Uhríčik, M., Markovičová, L., Pastierovičová, L. & Kuchariková, L. (2023). The Effect of Sensitization on the Susceptibility of AISI 316L Biomaterial to Pitting Corrosion. Materials, 16(16), 5714.
[15] Das Banik, S., Kumar, S., Singh, P. K. & Bhattacharya, S. (2023). Influence of weld repair on the residual stresses induced in austenitic stainless steel weld joints. Production Engineering, 17(1), 81-94.

[16] Djeloud, H., Moussaoui, M., Kouider, R., Al-Kassir, A. & Carrasco-Amador, J. P. (2023). Study of the heat exchange and relaxation conditions of residual stresses due to welding of austenitic stainless steel. Energies, 16(7), 3176.
[17] Rhodes, P. R. (1969). Mechanism of chloride stress corrosion cracking of austenitic stainless steels. Corrosion, 25(11), 462-472.
[18] Wells, D. B., Stewart, J., Davidson, R., Scott, P. M., & Williams, D. E. (1992). The mechanism of intergranular stress corrosion cracking of sensitised austenitic stainless steel in dilute thiosulphate solution. Corrosion Science, 33(1), 39-71.